J Appl Electrochem (2013) 43:575–582
DOI 10.1007/s10800-013-0545-2

ORIGINAL PAPER

# Phosphomolybdic acid modified PtRu nanocatalysts for methanol electro-oxidation

**Weimin Chen · Xufang Wei · Yu Zhang**

Received: 28 January 2013 / Accepted: 4 April 2013 / Published online: 20 April 2013


**Abstract** Phosphomolybdic acid ($H_3PMo_{12}O_{40}$, $PMo_{12}$) was employed to modify PtRu nanocatalysts for methanol electro-oxidation. The results show that the performance of PtRu catalysts was improved by the formation of the negatively charged self-assembled $PMo_{12}$ monolayer on the catalyst surface. Electrochemical measurements indicate that the $PMo_{12}$-modified PtRu catalyst has a higher catalytic activity and a better poison tolerance than the unmodified one. It is also found that the sequence in which PtRu and $PMo_{12}$ were deposited onto the carbon support during the preparation process has a major influence on the performance of $PMo_{12}$-modified PtRu nanocatalysts. X-ray photoelectron spectra results show that the self-assembled $PMo_{12}$ layer inhibits the formation of metal oxides/hydroxides on the surface of PtRu nanoparticles to some extent.

**Keywords** Direct methanol fuel cells · Electrocatalyst · Phosphomolybdic acid · Modification

## 1 Introduction

Direct methanol fuel cells (DMFCs) are considered to be promising potable power sources because of their advantages such as high energy densities, ambient operating conditions, as well as good portabilities [1, 2]. PtRu nanocatalysts are widely used as anode catalysts in DMFCs owing to the bi-functional effect [3]. Enormous efforts have been made to optimize the structure and composition of PtRu nanocatalysts, but so far, the activity and stability of the anode catalysts are still relatively low and need to be further improved. This is mainly due to the relatively poor kinetics of the methanol electro-oxidation on the anode and the poisoning of active sites caused by intermediates such as CO-like adsorbates formed during the dehydrogenation process of methanol [4–7]. It is necessary to develop an anode catalyst with a high activity for methanol dehydrogenation/oxidation and an improved tolerance to CO poisoning.

Polyoxometalates (POMs) are inorganic clusters with oxometalates that are outstanding in their topolog and electronic versatility characteristics [8]. Keggin-type POMs such as phosphomolybdic acid ($H_3PMo_{12}O_{40}$, abbreviated as $PMo_{12}$) are particularly attractive because of their ability to form the self-assembled monolayers on common solid electrode substrates [9–12]. $PMo_{12}$ has been used to improve the activity/stability of Pt-based nanocatalysts, and the promoting effect was ascribed to its excellent redox character, electronic versatility as well as high proton conductivity [13–17]. For carbon-supported PtRu nanocatalysts, the introduction of POMs gives rise to considerable changes in the surface structure. Therefore, it is necessary to investigate the relationship between the surface structure and the catalytic performance of the $PMo_{12}$-modified nanocatalyts. In this study, the influence of the self-assembled $PMo_{12}$ monolayer on the catalytic performance of PtRu nanocatalysts was examined. For comparison, two kinds of $PMo_{12}$-modified PtRu nanocatalysts were prepared. The difference between them is the sequence in which PtRu and $PMo_{12}$ were deposited onto the carbon support during the preparation process.

W. Chen (✉) · X. Wei · Y. Zhang
School of Environmental and Chemical Engineering, Shenyang Ligong University, Shenyang 110159, China
e-mail: cwmchem@163.com

## 2 Experimental

### 2.1 Preparation

The 30 wt% PtRu/C catalyst was synthesized using a $NaBH_4$ reduction method. The molar ratio of Pt to Ru is 1:1. Typically, 140 mg of carbon black (Vulcan XC-72, Cabot Corp.) was suspended in 50 mL of deionized water and stirred ultrasonically for 15 min; then 26.7 mL of hexachloroplatinic acid solution (1.48 mg Pt per mL) and 13.5 mL of ruthenium trichloride solution (1.52 mg Ru per mL) were added into the suspension dropwise. Afterward, 1.0 mol $L^{-1}$ NaOH solution was added to adjust the pH of the suspension to about 10. Adequate amount of $NaBH_4$ solution was added to reduce the PtRu precursors at 60 °C for 2 h. The suspension was filtered and washed with 2.5 L of deionized water and vacuumdried at 70 °C for 12 h.

Two kinds of $PMo_{12}$-modified PtRu nanocatalysts denoted as PtRu/$PMo_{12}$/C and $PMo_{12}$/PtRu/C were prepared. The only difference between them is the sequence in which PtRu and $PMo_{12}$ were deposited onto the carbon support during the preparation process. PtRu/$PMo_{12}$/C was prepared in the same way as PtRu/C, except that before the addition of PtRu precursors, 3.8 mL of phosphomolybdic acid solution (1.02 mg Mo per mL) was added into the carbon black suspension, and the mixture was stirred for 8 h. $PMo_{12}$/PtRu/C was prepared also in the same way as PtRu/C, except that after the deposition/reduction of PtRu precursors, 3.8 mL of phosphomolybdic acid solution (1.02 mg Mo per mL) was added into the suspension, and the mixture was stirred for 8 h.

### 2.2 Characterization

Electrochemical measurements were carried out at 25 °C, using a three-electrode system, in which the glassy carbon, the platinum foil, and the saturated calomel electrode (SCE) were used as the working electrode, the counter electrode, and the reference electrode, respectively. Catalyst inks were made by mixing 5 mg of the catalyst with 50 μL of 5 wt% Nafion® ionomer solution (EW = 1100, DuPont Corp.) and 1 mL of ethanol ultrasonically for 30 min. In electrode preparation, 25 μL of the prepared catalyst slurry was pipetted onto a glassy carbon electrode with a diameter of 4 mm (the geometric area is 0.126 $cm^2$), and the solvent was evaporated. Electrochemical measurements were conducted using a PAR2273 potentiostat/galvanostat. All potential values mentioned in this study were referenced to the SCE.

Transmission electron microscopy (TEM) measurements were performed using a FEI Tecnai F20 field emission transmission electron microscope operating at 200 kV. The size distribution and the mean particle size of the electrocatalysts were obtained by measuring more than 200 particles from TEM images. X-ray photoelectron spectra (XPS) were collected on a Thermo VG ESCALAB250 multifunction surface analysis system with a monochromatic aluminum Kα (1,486.6 eV) X-ray source operating at 150 W.

## 3 Results and discussion

A schematic illustration of the preparation of $PMo_{12}$-modified PtRu nanocatalysts is shown in Fig. 1. As mentioned above, there are two kinds of $PMo_{12}$-modified PtRu/C catalysts, i.e., PtRu/$PMo_{12}$/C and $PMo_{12}$/PtRu/C. The only difference between them is the sequence in which PtRu and $PMo_{12}$ were deposited onto the carbon support during the preparation process. For $PMo_{12}$/PtRu/C, the deposition/reduction of PtRu precursors was before the formation of the self-assembled $PMo_{12}$ layer, while for PtRu/$PMo_{12}$/C, the sequence was opposite. Obviously, in $PMo_{12}$/PtRu/C, PtRu nanoparticles were in direct contact with the carbon support, whereas in PtRu/$PMo_{12}$/C, the contact between the PtRu nanoparticle and the carbon support may be prevented to some degree because of the existence of the self-assembled $PMo_{12}$ monolayer.

Cyclic voltammetry (CV) curves of catalysts for methanol electro-oxidation are shown in Fig. 2. It is clearly seen that PtRu/$PMo_{12}$/C exhibits a much lower catalytic activity compared with PtRu/C. In contrast, $PMo_{12}$/PtRu/C displays a higher catalytic activity than PtRu/C. This result can be explained by the difference in the surface structure between PtRu/$PMo_{12}$/C and $PMo_{12}$/PtRu/C. As described above, in $PMo_{12}$/PtRu/C, PtRu nanoparticles were in direct contact with the carbon support, while in PtRu/$PMo_{12}$/C, the contact between the PtRu nanoparticle and the carbon support was prevented to some extent because of the existence of the self-assembled $PMo_{12}$ monolayer. Because $PMo_{12}$ monolayer is a good proton conductor but a somewhat poor electron conductor, it is inferred that the electron transfer from PtRu nanoparticles to the carbon support during the methanol electro-oxidation process was inhibited to some extent, resulting in a considerable activity-loss in PtRu/$PMo_{12}$/C. On the other hand, the higher catalytic activity in $PMo_{12}$/PtRu/C may be ascribed to the interaction between the PtRu nanoparticle and the self-assembled $PMo_{12}$ layer [12].

Another noteworthy phenomenon in Fig. 2 is that in PtRu/$PMo_{12}$/C and $PMo_{12}$/PtRu/C, the areas of the hydrogen adsorption/desorption peaks (within the potential region of approximately −0.24 – 0.06 V vs. SCE) are considerably smaller than that in PtRu/C. This observation likely suggests that the introduction of $PMo_{12}$ changed the surface structure of the carbon-supported PtRu catalyst and inhibited the hydrogen adsorption/desorption to some extent.

Fig. 1 Schematic illustration of the synthesis procedures of $PMo_{12}$-modified PtRu nanocatalysts

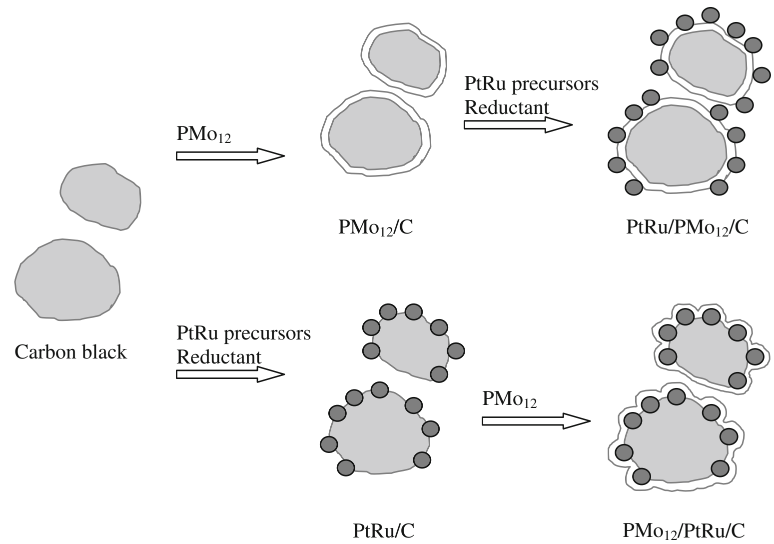


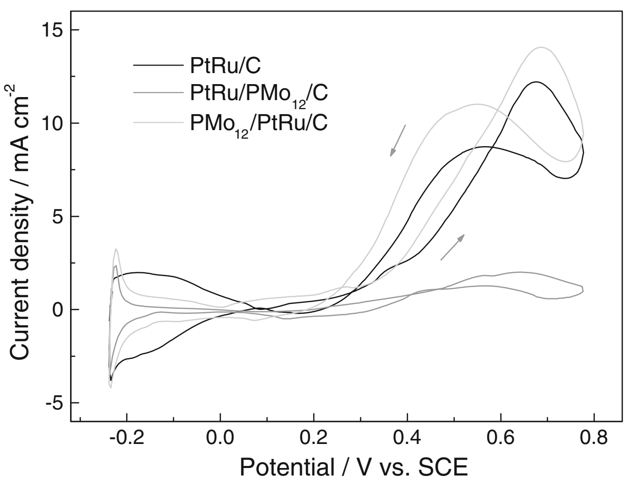


**Fig. 2** CV curves of catalysts in 0.5 mol $L^{-1}$ $H_2SO_4$–0.5 mol $L^{-1}$ $CH_3OH$ solution. Scan rate: 20 mV $s^{-1}$. *Inset* part of the CV curves in the forward scan

Figure 3 shows the linear sweep voltammetry (LSV) curves of catalysts. It is seen that within the low-potential region (approximately 0.22–0.37 V vs. SCE), the current density in $PMo_{12}$/PtRu/C is considerably higher than that in PtRu/C. It has been reported that the addition of phosphomolybdic acid improves the catalytic activity of PtRu catalysts toward methanol oxidation by means of the high particle dispersion [15, 16] and the co-catalytic effect [14]. With the increase in the potential, the ohmic resistance and the mass transfer resistance play more and more important roles in the catalytic performance; thus the current density reaches its peak value at approximately 0.55–0.58 V versus SCE. The poor catalytic activity in PtRu/$PMo_{12}$/C can also be attributed to the surface structure of PtRu/$PMo_{12}$/C, which inhibits the electron transfer from PtRu nanoparticles to the carbon support, as mentioned above.

The electrochemical impedance spectra (EIS) of catalysts in 0.5 mol $L^{-1}$ $H_2SO_4$–0.5 mol $L^{-1}$ $CH_3OH$ solution are shown in Fig. 4. Impedance spectra were recorded at five points per decade by superimposing a 5 mV ac signal on the cell under potentiostatic mode over the frequency range from 100 kHz to 0.1 Hz. The applied potential value is 0.5 V versus SCE. It is seen that in each catalyst, the Nyquist diagram consists of two arcs. The small arc that appears at the high-frequency range relates to electrical conduction via the electrical double layer or via geometric boundaries [18, 19]. The arc that appears at the low-frequency range relates to the electro-oxidation of methanol, and at the low-frequency end, this arc extends into the fourth quadrant and forms an induction loop that represents the electro-oxidation of $(CO)_{ads}$ [20, 21].

As shown in Fig. 4, the relatively small low-frequency arc in $PMo_{12}$/PtRu/C likely suggests that the methanol

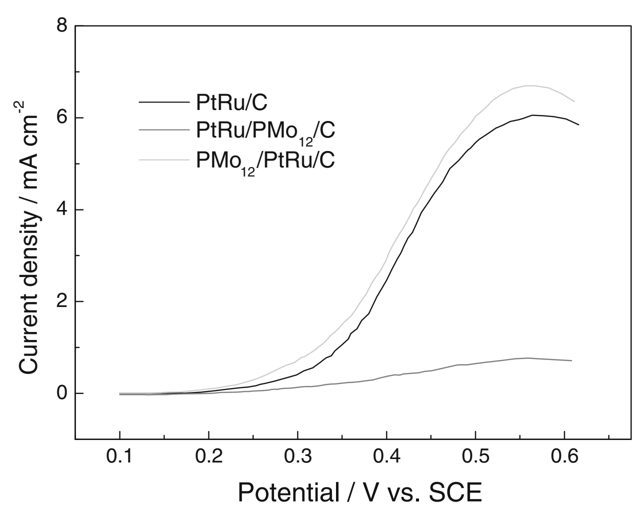


**Fig. 3** LSV curves of catalysts in 0.5 mol $L^{-1}$ $H_2SO_4$–0.5 mol $L^{-1}$ $CH_3OH$ solution. Scan rate: 1 mV $s^{-1}$

electro-oxidation reaction occurs more easily on $PMo_{12}$/PtRu/C than on PtRu/C. In contrast, the large low-frequency arc in PtRu/$PMo_{12}$/C implies that it is difficult for the reaction to take place on PtRu/$PMo_{12}$/C. It is also noticeable that the pure ohmic resistance (which can be derived from the intersection of the higher frequency arc on the real axis) in PtRu/$PMo_{12}$/C is measured to be 1.35 Ω $cm^2$, higher than that in PtRu/C (1.28 Ω $cm^2$) and $PMo_{12}$/PtRu/C (1.29 Ω $cm^2$). This result supports the assumption that in PtRu/$PMo_{12}$/C, the electron transfer from PtRu nanoparticles to the carbon support during the methanol electro-oxidation process was inhibited to some extent because of the formation of the $PMo_{12}$ layer.

Chronoamperometry tests were conducted to evaluate the poison resistance of catalysts. The applied potential was 0.5 V versus SCE. As shown in Fig. 5, at the beginning stage (0–10 min), there were rapid decreases in current density for all catalysts, which could be largely attributed to the rapid formation of metal oxides/hydroxides on the PtRu surface due to the exposure of the catalysts to a high potential. These metal oxides/hydroxides covered the active sites on the catalyst surface, thus decreasing the catalytic activity. Besides, the accumulation of intermediates on the catalyst surface may also contribute to the rapid current decay. Because the current density in PtRu/$PMo_{12}$/C is significantly lower than that in the others, any discussion about the poison resistances of this catalyst is meaningless. Within the time span of 10–30 min, PtRu/C lost 65.2 % of its original catalytic activity, while $PMo_{12}$/PtRu/C lost only 49.8 % of its original catalytic activity. Obviously, $PMo_{12}$/PtRu/C exhibits a considerable lower activity-loss rate than PtRu/C, which could be largely ascribed to the poison-removal ability of $PMo_{12}$. It has been demonstrated that Keggin-type $PMo_{12}O_{40}{}^{3-}$ anions in an aqueous solution could effectively assist the electrochemical oxidation of carbon monoxide (CO) with water molecules to carbon dioxide ($CO_2$) over gold catalysts [13, 22], as represented by

$$CO(g) + H_2O(l) + PMo_{12}O_{40}^{3-}(aq) \rightarrow CO_2(g) + 2H^+(aq) + PMo_{12}O_{40}^{5-}(aq) \quad (1)$$

It is well known that CO-like adsorbates are representative of intermediate products in the methanol electro-oxidation reaction and those adsorbates often cause catalyst poisonings, so the higher poison resistance in $PMo_{12}$/PtRu/C than in PtRu/C is likely due to the poison-removal ability of $PMo_{12}$. In addition, the coverage of the PtRu nanoparticles by the self-assembled $PMo_{12}$ monolayer may also contribute to the high electrochemical stability of $PMo_{12}$/PtRu/C. Han and co-workers [15, 16] reported that the negatively charged $PMo_{12}$ monolayer effectively prevented the agglomeration of PtRu nanoparticles by the electrostatic repulsive effect. It is also suggested that the negatively charged $PMo_{12}$ layer may prevent the migration of complex metal anions along the catalyst surface by the electrostatic repulsive effect and thus inhibit the dissolution of active species from PtRu nanoparticles to some extent.

TEM images of catalysts are shown in Fig. 6. It is noticeable that the morphologies of PtRu/$PMo_{12}$/C (Fig. 6b) and $PMo_{12}$/PtRu/C (Fig. 6c) are different from that of PtRu/C (Fig. 6a). From Fig. 6b and c, it is clearly seen that the catalyst masses are surrounded by light shells, which are considered to originate from the self-assembled phosphomolybdic acid layer [23]. It is also seen that the TEM images of PtRu/$PMo_{12}$/C (Fig. 6b) and $PMo_{12}$/PtRu/C (Fig. 6c) look somewhat similar. It is presented tp be so because in TEM images, the $PMo_{12}$ layers (light shells) are very prominent, whereas the PtRu nanoparticles are dark

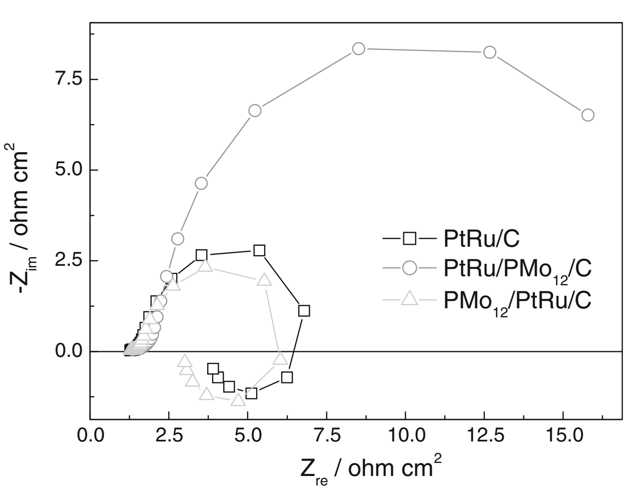


**Fig. 4** EIS spectra of catalysts in 0.5 mol $L^{-1}$ $H_2SO_4$–0.5 mol $L^{-1}$ $CH_3OH$ solution. Applied potential: 0.5 V versus SCE

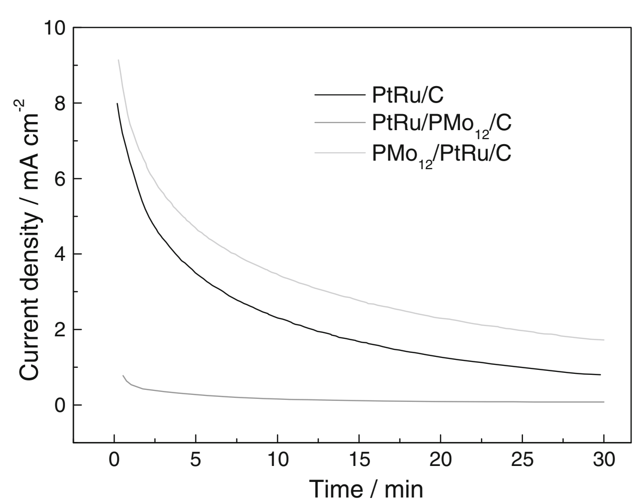


**Fig. 5** Chronoamperometry curves of catalysts in 0.5 mol $L^{-1}$ $H_2SO_4$–0.5 mol $L^{-1}$ $CH_3OH$ solution. Potential: 0.5 V versus SCE

and their boundaries cannot be clearly seen. Therefore the difference in the layer structure between PtRu/$PMo_{12}$/C and $PMo_{12}$/PtRu/C cannot be clearly distinguished in the TEM images. The mean particle sizes of PtRu/C, PtRu/$PMo_{12}$/C, and $PMo_{12}$/PtRu/C are measured to be 2.9, 3.1, and 2.8 nm, respectively. PtRu/$PMo_{12}$/C shows some degree of agglomeration, which could be explained by its unique surface structure: in PtRu/$PMo_{12}$/C, PtRu nanoparticles are loaded on the self-assembled $PMo_{12}$ layer rather than on the carbon support; thus the chelating effect between the PtRu nanoparticle and the surface functional group of the carbon support is much weaker in PtRu/$PMo_{12}$/C than that in PtRu/C and $PMo_{12}$/PtRu/C.

X-ray photoelectron spectra of catalysts were collected to investigate the interaction between the PtRu nanoparticle and the $PMo_{12}$ monolayer. Before the data were corrected based on the C 1s value of 284.6 eV, it is observed that the binding energy values in the uncorrected XPS spectra of PtRu/$PMo_{12}$/C and $PMo_{12}$/PtRu/C were considerably lower than those in the uncorrected XPS spectra of PtRu/C, as shown in Fig. 7. This tendency can be more clearly seen from the position of C 1s peaks in the uncorrected XPS spectra, as shown in the inset of Fig. 7. The low binding energy values in the uncorrected XPS spectra of PtRu/$PMo_{12}$/C and $PMo_{12}$/PtRu/C can be ascribed to the minus electric field established by negatively charged Keggin-type $PMo_{12}O_{40}^{3-}$ anions in the self-assembled $PMo_{12}$ layer. In order to investigate the chemical states of active species on the catalyst surface, XPS spectra were corrected with the binding energies of XPS peaks referenced to the C 1s value of 284.6 eV.

Figure 8 shows the O 1s XPS spectra of catalysts. It is seen that the O 1s spectra appear to be composed of noble/transition metal oxides (531.0 eV) and the hydroxides (532.8 eV). The relative ratios of different O 1s species are listed in Table 1. The results show that the dominant O species on the surface of $PMo_{12}$/PtRu/C is remarkably different from that on the surfaces of PtRu/C and PtRu/$PMo_{12}$/C. The relative intensity of metal hydroxides on the surface of $PMo_{12}$/PtRu/C is 49.0 %, much lower than that on the surface of PtRu/C (63.3 %) and PtRu/$PMo_{12}$/C (69.8 %). This result likely suggests that the dominant surface O species on the surface of $PMo_{12}$/PtRu/C is oxygen in the Keggin-type $PMo_{12}$ structure, while the dominant surface O species on the surfaces of PtRu/C and PtRu/$PMo_{12}$/C is oxygen in the forms of PtRu oxides/hydroxides. This observation confirms the difference in the surface structure between PtRu/$PMo_{12}$/C and $PMo_{12}$/PtRu/C.

Chemical states of Pt on the surface of catalysts are investigated by deconvolution of the Pt 4f XPS spectra, as shown in Fig. 9, and the analysis results are listed in Table 1. Pt exists in different chemical states in the catalysts. The

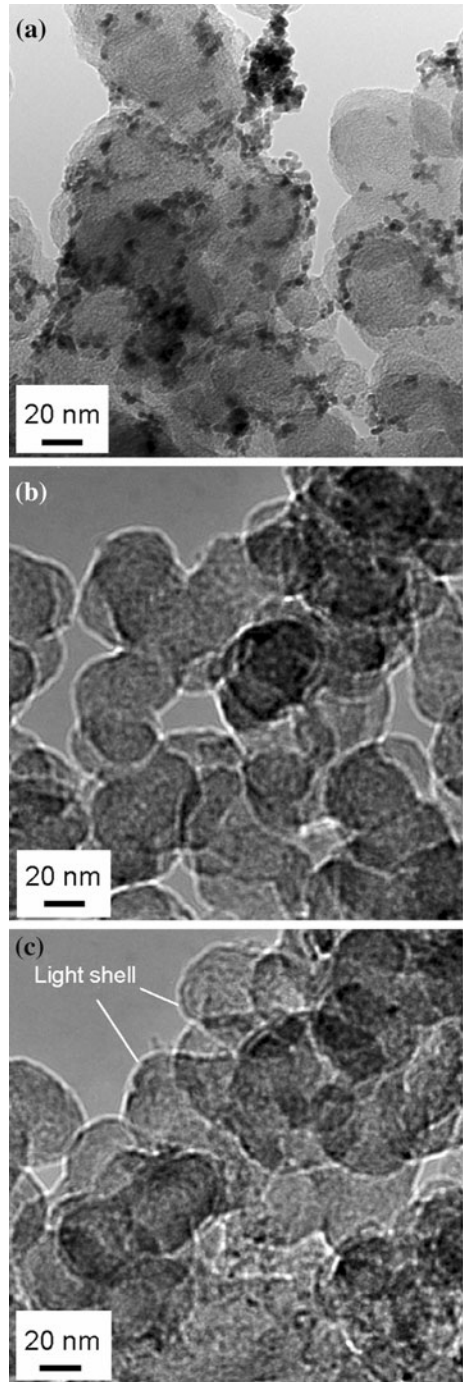


**Fig. 6** TEM images of catalyst samples: **a** PtRu/C, **b** PtRu/$PMo_{12}$/C, **c** $PMo_{12}$/PtRu/C

most intense doublet (71.6 and 74.9 eV) is attributed to metallic platinum Pt(0). The second doublet (72.8 and 76.1 eV) is assigned to Pt(II) species such as PtO and $Pt(OH)_2$. The third doublet (74.7 and 78.0 eV) could be assigned to Pt species in a higher chemical state such as $PtO_2$ and other Pt(IV) species adsorbed on the metal surface.

Table 1 shows that the relative intensity of metallic species Pt(0) in $PMo_{12}$/PtRu/C is 64.4 %, which is higher

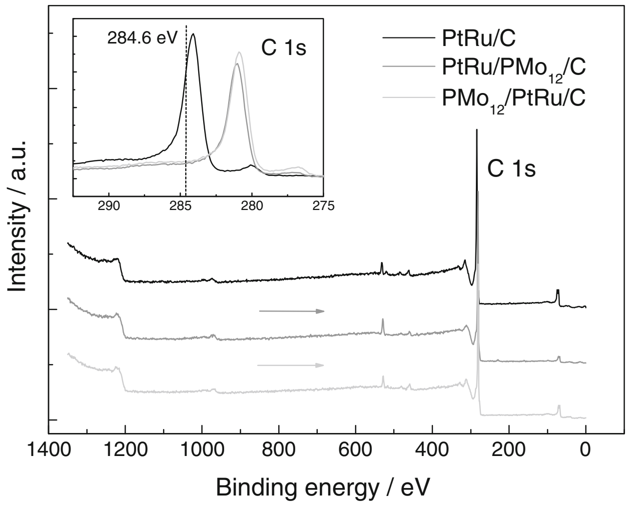


**Fig. 7** Uncorrected survey XPS spectra of catalyst samples. *Inset* C 1s peaks in the uncorrected survey XPS spectra of catalyst samples

than that in PtRu/C (56.1 %) and that in PtRu/$PMo_{12}$/C (43.1 %). It is well known that XPS is a surface analysis technique. In $PMo_{12}$/PtRu/C, the surface of the PtRu nanoparticle is covered with a self-assembled $PMo_{12}$ layer, and so the high surface content of Pt(0) in $PMo_{12}$/PtRu/C could be ascribed to the synergetic effect between the Pt nanoparticle and the $PMo_{12}$ layer. This observation is in good agreement with Chojak and co-workers' results [24]. They found that the presence of the polyoxometallate monolayer on platinum results in the partial suppression of the interfacial formation of PtOH/PtO oxides, and the existence of sufficient by uncovered active sites on the metal surface facilitates the methanol electro-oxidation reaction.

Owing to severe interferences caused by the overlapping of the Ru 3d and C 1s XPS spectra, the less-intense Ru 3p XPS spectra of catalysts were used to study the surface compositions of catalysts, as shown in Fig. 10. The Ru 3p peaks are deconvoluted and assigned into three sets of doublets with Ru $3p_{3/2}$ centered at binding energy 461.7 (Ru(0)), 463.1 ($RuO_2$), and 465.2 eV ($RuO_xH_y$). Table 1 shows that the surface content of metallic ruthenium Ru(0) in $PMo_{12}$/PtRu/C is 48.9 % which is, higher than those in PtRu/C (48.1 %) and PtRu/$PMo_{12}$/C (38.3 %). It is suggested that the sufficient metallic species on the catalyst surface contribute to the high catalytic activity and the good poison resistance of $PMo_{12}$/PtRu/C for the methanol-oxidation reaction.

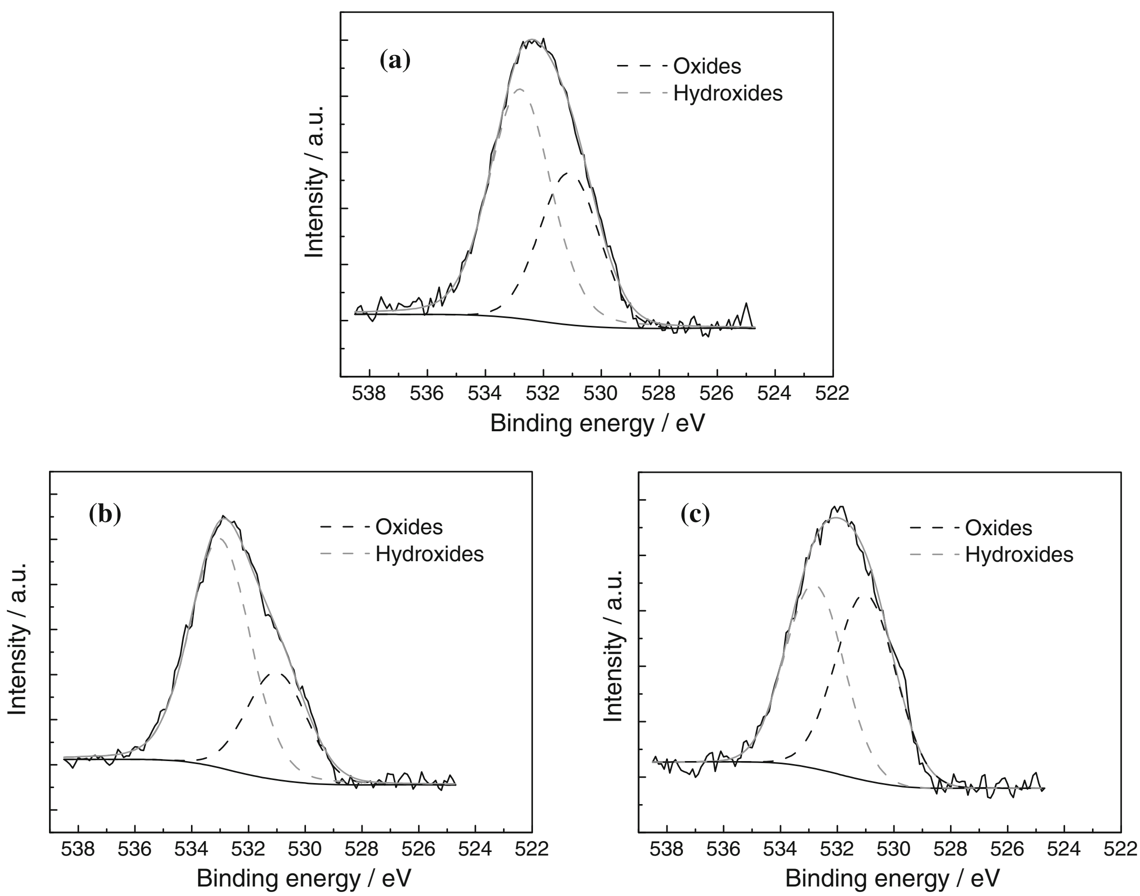


**Fig. 8** O 1s region of XPS spectra of catalyst samples: **a** PtRu/C, **b** PtRu/$PMo_{12}$/C, **c** $PMo_{12}$/PtRu/C

**Table 1** Curve-fitting results of the XPS spectra

| Electrocatalysts | Pt $4f_{7/2}$ | | Ru $3p_{3/2}$ | | O 1s | |
|---|---|---|---|---|---|---|
| | Binding energy (eV) | Relative ratio (%) | Binding energy (eV) | Relative ratio (%) | Binding energy (eV) | Relative ratio (%) |
| PtRu/C | 71.6 | 56.1 | 461.7 | 48.1 | 531.1 | 36.7 |
| | 72.8 | 30.3 | 463.1 | 35.6 | 532.8 | 63.3 |
| | 74.7 | 13.6 | 465.2 | 16.3 | | |
| PtRu/$PMo_{12}$/C | 71.7 | 43.1 | 461.7 | 38.3 | 531.0 | 30.2 |
| | 72.9 | 31.3 | 463.1 | 38.3 | 533.0 | 69.8 |
| | 74.8 | 25.6 | 465.2 | 23.4 | | |
| $PMo_{12}$/PtRu/C | 71.5 | 64.4 | 461.7 | 48.9 | 531.0 | 51.0 |
| | 72.7 | 12.5 | 463.1 | 35.1 | 532.8 | 49.0 |
| | 74.6 | 23.1 | 465.2 | 16.0 | | |

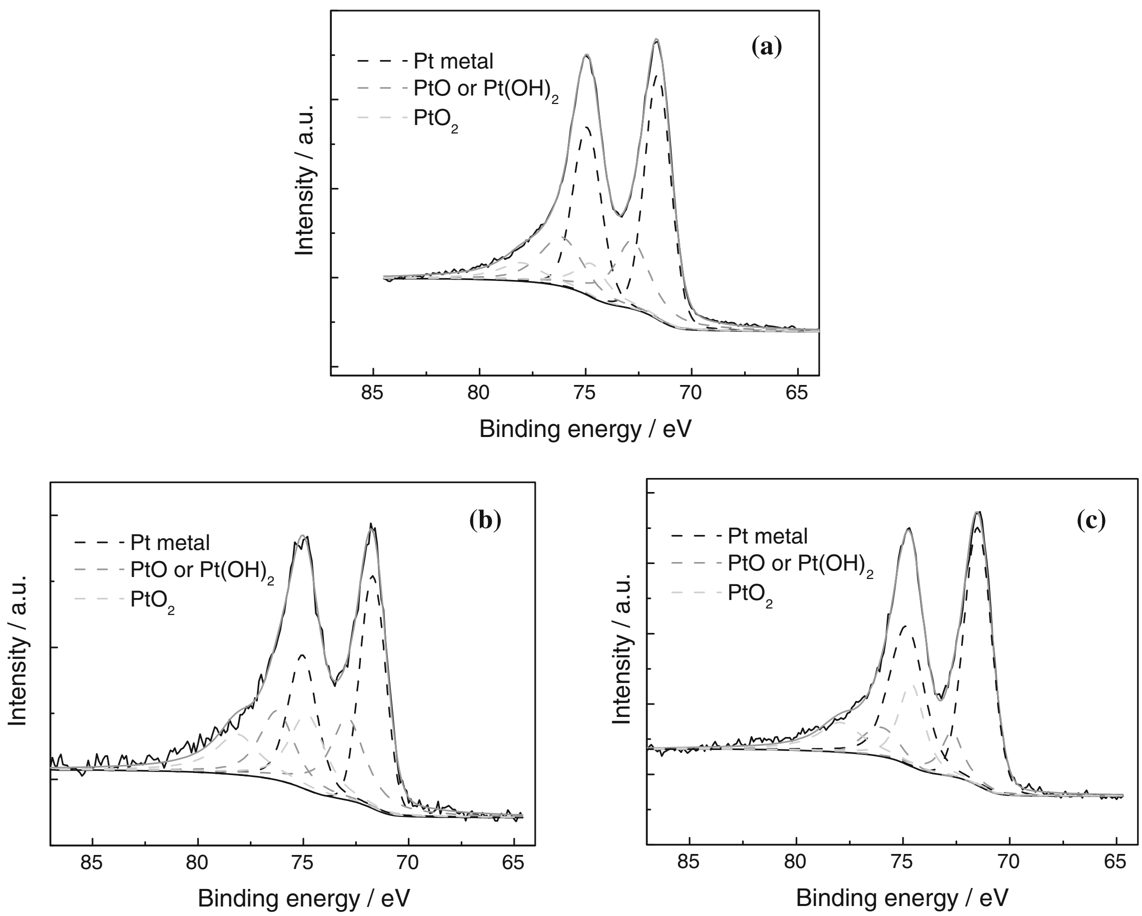


**Fig. 9** Pt 4f region of XPS spectra of catalyst samples: **a** PtRu/C, **b** PtRu/$PMo_{12}$/C, **c** $PMo_{12}$/PtRu/C

## 4 Conclusions

The performances of PtRu catalysts are improved by the formation of negatively charged self-assembled $PMo_{12}$ layers on the surface. The sequence in which PtRu and $PMo_{12}$ were deposited onto the carbon support during the preparation has a major influence on the catalytic performance of $PMo_{12}$-modified PtRu nanocatalysts. The self-assembled $PMo_{12}$ layer inhibits the formation of metal oxides/hydroxides on the surface of PtRu nanoparticles to

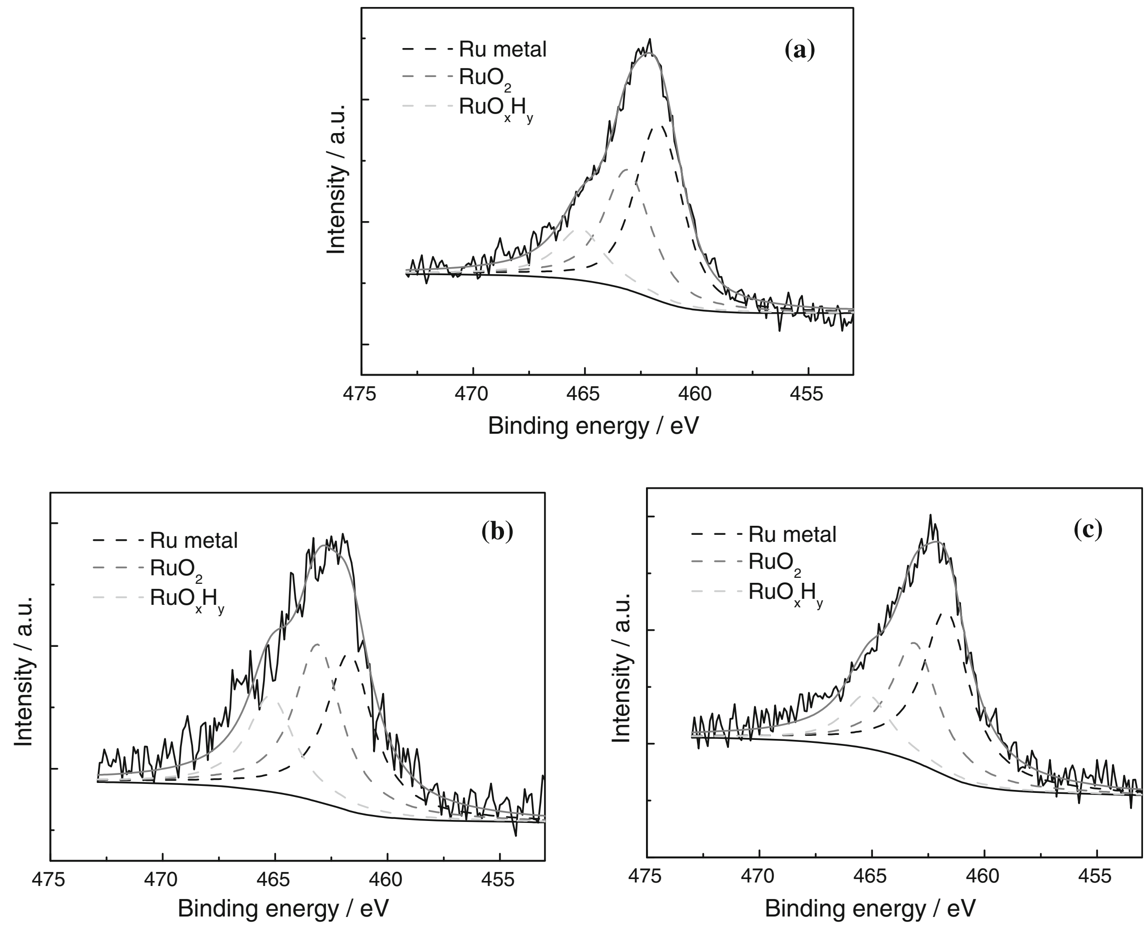


**Fig. 10** Ru $3p_{3/2}$ region of XPS spectra of catalyst samples: **a** PtRu/C, **b** PtRu/$PMo_{12}$/C, **c** $PMo_{12}$/PtRu/C

some extent. $PMo_{12}$ modification is an effective means of improving the catalytic activity and the poison-tolerance ability of PtRu nanocatalysts for methanol electro-oxidation.

**Acknowledgments** This study was financially supported by the National Natural Science Foundation of China (Grant No. 21273152 and 51004072).

## References


1. Aricò AS, Srinivasan S, Antonucci V (2001) Fuel Cells 1(2):133
2. Gottesfeld S (2007) J Power Sources 171(1):37
3. Watanabe M, Motoo S (1975) J Electroanal Chem 60(3):267
4. Seiler T, Savinova ER, Friedrich KA et al (2004) Electrochim Acta 49(22–23):3927
5. Lu GQ, Chrzanowski W, Wieckowski A (2000) J Phys Chem B 104(23):5566
6. Waszczuk P, Solla-Gullón J, Kim HS et al (2001) J Catal 203(1):1
7. Gojković SLJ, Vidaković TR, Đurović DR (2003) Electrochim Acta 48(24):3607
8. Pope MT, Muller A (1991) Angew Chem Int Ed 30(1):34
9. Pan DW, Chen JH, Tao WY et al (2006) Langmuir 22(13):5872
10. Garrigue P, Delville MH, Labrugère C et al (2004) Chem Mater 16(16):2984
11. Cui Z, Kulesza PJ, Li CM (2011) Int J Hydrogen Energy 36(14):8508
12. Wang D, Lu S, Xiang Y et al (2011) Appl Catal B 103(3–4):311
13. Seo MH, Choi SM, Kim HJ et al (2008) J Power Sources 179(1):81
14. Ferrell JR III, Kuo KC, Turner JA et al (2008) Electrochim Acta 53(14):4927
15. Han DM, Guo ZP, Zhao ZW et al (2008) J Power Sources 184(2):361
16. Guo ZP, Han DM, Wexler D et al (2008) Electrochim Acta 53(22):6410
17. Guo X, Guo DJ, Wang JS et al (2010) J Electroanal Chem 638(1):167
18. Otomo J, Li X, Kobayashi T et al (2004) J Electroanal Chem 573:99
19. Mueller JT, Urban PM (1998) J Power Sources 75:139
20. Müller JT, Urban PM, Hölderich WF (1999) J Power Sources 84:157
21. Hsing IM, Wang X, Leng YJ (2002) J Electrochem Soc 149(5):A615
22. Kim WB, Voitl T, Rodriguez-Rivera GJ (2004) Science 305(5688):1280
23. Kulesza PJ, Chojak M, Karnicka K et al (2004) Chem Mater 16(21):4128
24. Chojak M, Kolary-Zurowska A, Wlodarczyk R et al (2007) Electrochim Acta 52(18):5574